Available online at www.sciencedirect.com
SCIENCE DIRECT
Brain Research 1057 (2005) 98 – 104
BRAIN RESEARCH
www.elsevier.com/locate/brainres

Research Report

Rostro-caudal variations in neuronal size reflect the topography of cellular phenotypes in the rat superior cervical sympathetic ganglion

Drew B. Headley, Nadine M. Suhan, John P. Horn*

Department of Neurobiology, University of Pittsburgh School of Medicine, E1440 Biomedical Science Tower, Pittsburgh, PA 15261, USA

Accepted 19 July 2005
Available online 19 August 2005

Abstract

The mammalian superior cervical ganglion (SCG) contains a complex mixture of neuronal phenotypes that selectively innervate different peripheral targets. The present study examined the rostro-caudal topography of sympathetic phenotypes in the rat SCG by analyzing the relation between cell position, size, and the expression of immunoreactivity for neuropeptide Y (NPY), calretinin, and calcitonin gene-related peptide (CGRP). We observed that 64% of SCG neurons expressed NPY and had an average diameter of ~24 μm throughout the ganglion. Previous studies indicate that most of these cells are vasoconstrictor in function. By contrast, the size of NPY-negative neurons varied from ~25 μm in the rostral ganglion near the internal carotid nerve to ~30 μm in the caudal ganglion between the external carotid nerve and cervical sympathetic trunk. Many of the large NPY-negative neurons in the caudal ganglion were surrounded by dense axonal baskets that were immunoreactive for calretinin and therefore are likely to be secretomotor neurons projecting to salivary glands. Consistent with earlier reports, the rostral ganglion contained low numbers of presumptive pupillomotor neurons, based on their expression of NPY and contact with fibers containing CGRP. The present results indicate that neuronal size may provide a useful aid to cellular identification, especially in the caudal ganglion, and they provide further evidence of a topographic organization within the mammalian SCG.

Theme: Endocrine and autonomic regulation
Topic: Cardiovascular regulation

Keywords: Sympathetic neuron; Vasomotor; Pilomotor; Secretomotor; Pupillomotor; Neuropeptide Y; Calcitonin gene-related peptide; Calretinin

1. Introduction

Distinct subsets of sympathetic neurons selectively innervate different peripheral targets [8,11,20]. Although functional specificity thus serves as the primary criterion for classification of vasoconstrictor, piloerector, and secretomotor neurons, these and other sympathetic phenotypes can also be distinguished by additional specialized properties. Such markers may include the cell-type-specific expression of ion channels, neuropeptides, and molecules related to synaptic signaling [1,9,11,13,14]. The present study examines whether neuronal size and position are practical criteria for cellular identification in the rat superior cervical ganglion (SCG). The availability of such criteria would facilitate physiological studies of identified neurons. As a first step in approaching this problem, we compared at three positions along the rostro-caudal axis of the SCG the sizes of neurons expressing neuropeptide Y (NPY) and their relation to preganglionic fiber groups that express calretinin and calcitonin gene-related peptide (CGRP).

The clearest precedent for cell size as a marker of sympathetic phenotypes comes from studies of amphibian paravertebral ganglia nine and ten [7,18,26]. In toads and frogs, ganglia nine and ten form the caudal end of the sympathetic chain and they contain two major phenotypes. Secretomotor B neurons and vasomotor C neurons are distinguished not only by their functionality [23,30], but also by different axonal spike conduction velocities [7,26] and by expression of different neuropeptides [16,17,25] and different muscarinic synaptic mechanisms [16,19,28,29]. On average, vasomotor C neurons are 24% smaller in diameter

* Corresponding author. Fax: +1 412 648 1441.
E-mail address: jph@pitt.edu (J.P. Horn).

0006-8993/$ - see front matter © 2005 Elsevier B.V. All rights reserved.
doi:10.1016/j.brainres.2005.07.029

than secretomotor B neurons [7] and C neurons can be reliably identified by their selective expression of NPY [17].

The structure of NPY is highly conserved from elasmobranchs up through man [2,5,24] and its expression provides a link between cell identification in amphibian and mammalian sympathetic ganglia. As in amphibians, approximately 50–65% of mammalian sympathetic neurons express NPY and most of these neurons are involved in cardiovascular control [11,21]. However, the analysis of cellular identity is more complicated in mammals because SCG neurons express greater phenotypic diversity. Approximately 90% of SCG neurons can be accounted for by three large groups of cells consisting of NPY-positive vasomotor neurons, NPY-negative pilomotor neurons, and NPY-negative secretomotor neurons projecting to the submandibular salivary glands [8,10,11,31]. The remaining small groups of SCG neurons include NPY-positive neurons projecting to the pineal gland [4,27] and eye [6,15]. The possibility that measurements of neuronal size could help to sort out the major differences between these cell groups was first demonstrated in the mouse SCG with experiments that combined immunocytochemistry with retrograde labeling methods [10]. In this work, NPY-positive neurons were found to be primarily vasoconstrictor in function, among the smallest cells in the ganglion and smaller on the whole than NPY-negative neurons.

In the present experiments, we wanted first to determine whether cell size correlates with NPY expression in the rat SCG, as in amphibian and mouse ganglia. Our second goal was to determine whether the size of NPY-immunoreactive cells varied as a function of cell position along the rostro-caudal axis of the SCG. In principle, cell position could be important because the SCG is divided into two major zones demarcated by the external carotid nerve (ECN) [3]. Neurons located in the rostral SCG project by way of the internal carotid nerve (ICN) to the brain vasculature, orbit, pineal gland, and skin overlying the rostral head [4,8,10–12,15,27]. By contrast, neurons in the caudal SCG project by way of the ECN to vasculature of the mouth and jaw, skin overlying the caudal head, and to salivary glands [8,10,14,31]. From this cellular topography, one would predict that variations in the mix of neuronal phenotypes at different positions along the rostro-caudal axis of the ganglion are reflected in cellular-size profiles.

2. Materials and methods

2.1. Animals and tissue preparation

The data in this study were derived from fourteen adult Sprague–Dawley rats (twelve males, two females, 160–250 g) obtained from Charles River Laboratories. All procedures pertaining to the care and use of live animals were conducted in accord with a protocol approved by the Institutional Animal Care and Use Committee at the University of Pittsburgh.

Animals were euthanized by an overdose of isoflurane. This was followed immediately by transcardiac perfusion with 50 ml of phosphate buffered saline (PBS) that contained 10 mM phosphate buffer (PB) and 0.9% NaCl (pH = 7.3, room temperature) and then by perfusion with 250 ml of fixative that contained 2% paraformaldehyde and 0.2% picric acid in 0.1 M PB (pH = 7.3, room temperature). After the perfusion, both SCGs were immediately dissected, pinned out in a Sylgard-coated petri dish, desheathed, post-fixed for 1 h at room temperature, and rinsed with PBS. The isolated ganglia were then dehydrated through graded ethanols and infiltrated with polyethyleneglycol (PEG, MW = 1000, Sigma #P3515) for 30 min at 47 °C under vacuum [22]. Ganglia were then oriented longitudinally in an embedding mold filled with PEG (MW = 1450, Sigma #P5402) and allowed to harden in a −20 °C freezer for 10 min. Ten-micrometer serial sections were cut on a Leica RM 2165 microtome and stored at 4 °C in individual wells containing PBS with 0.02% sodium azide until further processing.

2.2. Immunocytochemistry

2.2.1. Neuropeptide Y and Nissl stain

Following five rinses in PBS, floating sections were incubated for 2 h at room temperature in a blocking buffer that contained 1.5% donkey serum (Jackson ImmunoResearch Laboratories) and 0.3% Triton X-100 (Sigma) in PBS. The sections were then incubated overnight at 4 °C in sheep anti-NPY serum (Novus Biologicals #ab6173) diluted 1:750 in blocking buffer. After five rinses in PBS, sections were incubated in CY2-conjugated donkey anti-sheep IgG (Jackson ImmunoResearch Laboratories) diluted 1:200 in blocking buffer for 1.5 to 2 h at room temperature. After three rinses in PBS, sections were counterstained for 20 min at room temperature with NeuroTrace red (Molecular Probes #N-21482) diluted 1:200 in blocking buffer. The sections were then rinsed three final times in PBS, mounted on glass slides, allowed to dry overnight, dehydrated through ethanols, cleared in xylenes and coverslipped using Krystalon (Harleco). To assure the adequacy of staining with the sheep anti-NPY serum, we compared it with sections processed with a rabbit anti-NPY serum (1:1,000, Peninsula Laboratories) followed by CY2-conjugated donkey anti-rabbit IgG (1:200, Jackson ImmunoResearch Laboratories).

2.2.2. Calretinin and NPY

For double labeling, sections were blocked in 1.5% donkey serum and 0.3% Triton X-100 in PBS for 1.5 h at room temperature. The sections were then incubated overnight at 4 °C in a mixture of primary antibodies-sheep anti-NPY (1:750) and rabbit anti-calretinin (1:1000, Chemicon International #ab5054). After brief rinses in PBS, the sections were incubated for 1.5 h in a mixture of CY2-

conjugated donkey anti-sheep and CY3-conjugated donkey anti-rabbit, both diluted 1:200 in blocking buffer, followed by rinsing, mounting, and coverslipping.

2.2.3. CGRP and NPY

Sections were processed with a mixture of sheep anti-NPY serum (1:750) and rabbit anti-CGRP (1:1000, Cambridge Research Biochemicals) using the same protocol and secondary antibodies described for NPY/calretinin immunostaining.

2.3. Microscopy and image analysis

Sections were viewed, photographed, and analyzed with a Zeiss Axioskop 2 microscope, AxioCam HRc digital camera, and Axiovision 4.2 software. For the positional analysis of NPY expression, we selected sections in which one could identify as landmarks either the cervical sympathetic trunk (CST), the external carotid nerve (ECN), or the internal carotid nerve (ICN). Fields of cells adjacent to these landmarks were then photographed with a 40× objective under epifluorescence illumination to record NPY expression (green) and Nissl staining (red). To eliminate double counting, we photographed alternate sections and only included neuronal profiles with nucleoli in the analysis. Each cell meeting these criteria was scored for immunoreactivity and the cell body perimeter was traced to measure its area using Axiovision. Equivalent diameters were calculated as $2\sqrt{(\text{area}/\pi)}$.

2.4. Statistics

The grand means of cell diameters for NPY-positive and NPY-negative neurons were compared using a 2-tailed, unpaired, t test. The existence of statistical differences between groups within this data set was then established using a 1-way ANOVA followed by Tukey's post test using Prism 4.0 (GraphPad). $P < 0.01$ was the criterion for statistical significance. Grouped data are expressed as the mean ± SD.

3. Results

Consistent with previous work [21], we observed numerous neuropeptide Y-immunoreactive (NPY-IR) neurons scattered among NPY-negative neurons throughout the entire rostro-caudal extent of the rat SCG (Fig. 1A). Often, the NPY-IR neurons were in small clusters or in short single-file rows, with densest cellular staining in the perinuclear cytoplasm (Fig. 1B). When neurons located near the cervical sympathetic trunk (CST), external carotid nerve (ECN), and internal carotid nerve (ICN) were sampled in 7 ganglia from 7 rats, 64% of 3789 neuronal profiles were immunoreactive for NPY. On average, the NPY-positive neurons were 4 μm smaller in diameter than NPY-negative neurons (24.1 ± 3.9 μm vs. 28.0 ± 5.4 μm, $P < 0.0001$, unpaired, two-tailed t test). Plotting the size data as cumulative probability histograms (Fig. 1C) also showed clear differences in their midpoints and slopes, which

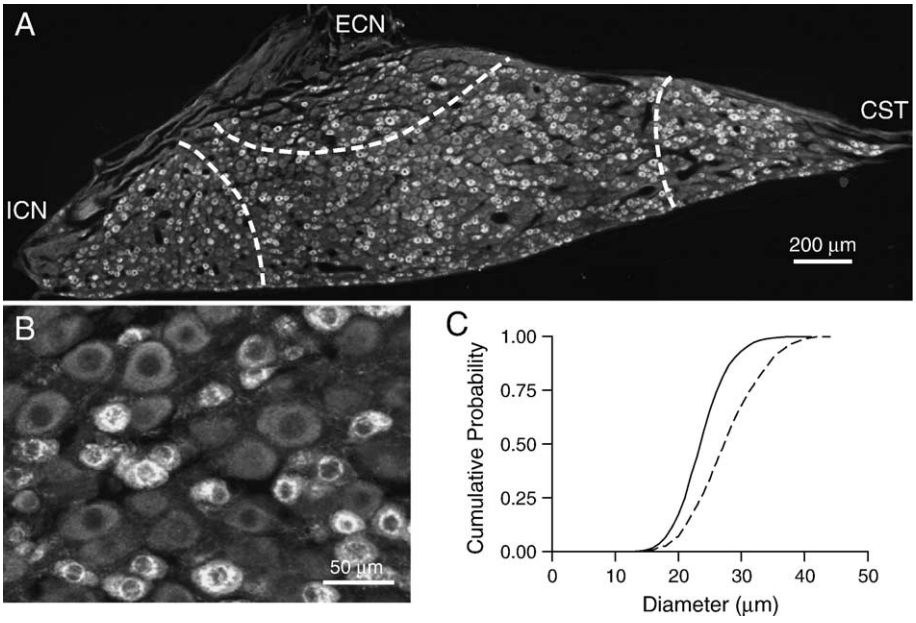

Fig. 1. NPY-positive sympathetic neurons are distributed throughout the entire superior cervical ganglion and are smaller than NPY-negative neurons. (A) Low-power montage of a section containing the CST, ECN, and ICN with the adjacent regions that were used for size analysis marked by dashed lines. By expanding the electronic version of this figure (Adobe PDF) to 400%, one can more easily see that the NPY-positive and NPY-negative cells tend to be in small interdigitated clusters. (B) Higher magnification of a field within panel A illustrates the classic perinuclear staining pattern for NPY-IR and the unambiguous distinction between immunoreactive and non-immunoreactive neurons. (C) Cumulative probability histograms of neuronal diameter show that NPY-IR neurons (solid line) are smaller than NPY-negative neurons (dashed line).

reflects the smaller median diameter and lower variability of NPY-positive neurons. One explanation for the greater variability of NPY-negative neurons is the presence of multiple cell groups having different sizes. To explore this possibility, the data for NPY-negative cells were binned and replotted as non-cumulative size histograms (not shown), which revealed hints of two or three peaks, consistent with the notion of overlapping subpopulations of cells. However, these peaks were not well resolved and their appearance proved sensitive to bin size. By presenting the data as cumulative histograms (Figs. 1–3), we avoided binning and assumptions about bin size.

Analyzing the size data (Fig. 1C) with reference to cell position revealed that the difference between NPY-positive and NPY-negative neurons varied along the rostro-caudal axis (Fig. 2, Table 1). At the rostral end of the ganglion, near the internal carotid nerve (ICN), NPY-positive neurons were only 1 μm smaller in diameter than NPY-negative neurons. This tiny difference was variable between animals, but statistically significant in the grouped data from 7 animals (Fig. 2, Table 1). In contrast, NPY-positive cells were ~6 μm smaller than NPY-negative cells at more caudal locations near the external carotid nerve (ECN) and the cervical sympathetic trunk (CST). Similarly, large differences in cell size were found at both caudal locations and were statistically significant, both in the grouped data (Fig. 2) and in each ganglion from 5 male and 2 female rats (Table 1).

Comparing the size distributions of NPY-positive neurons at the CST, ECN, and ICN revealed that they

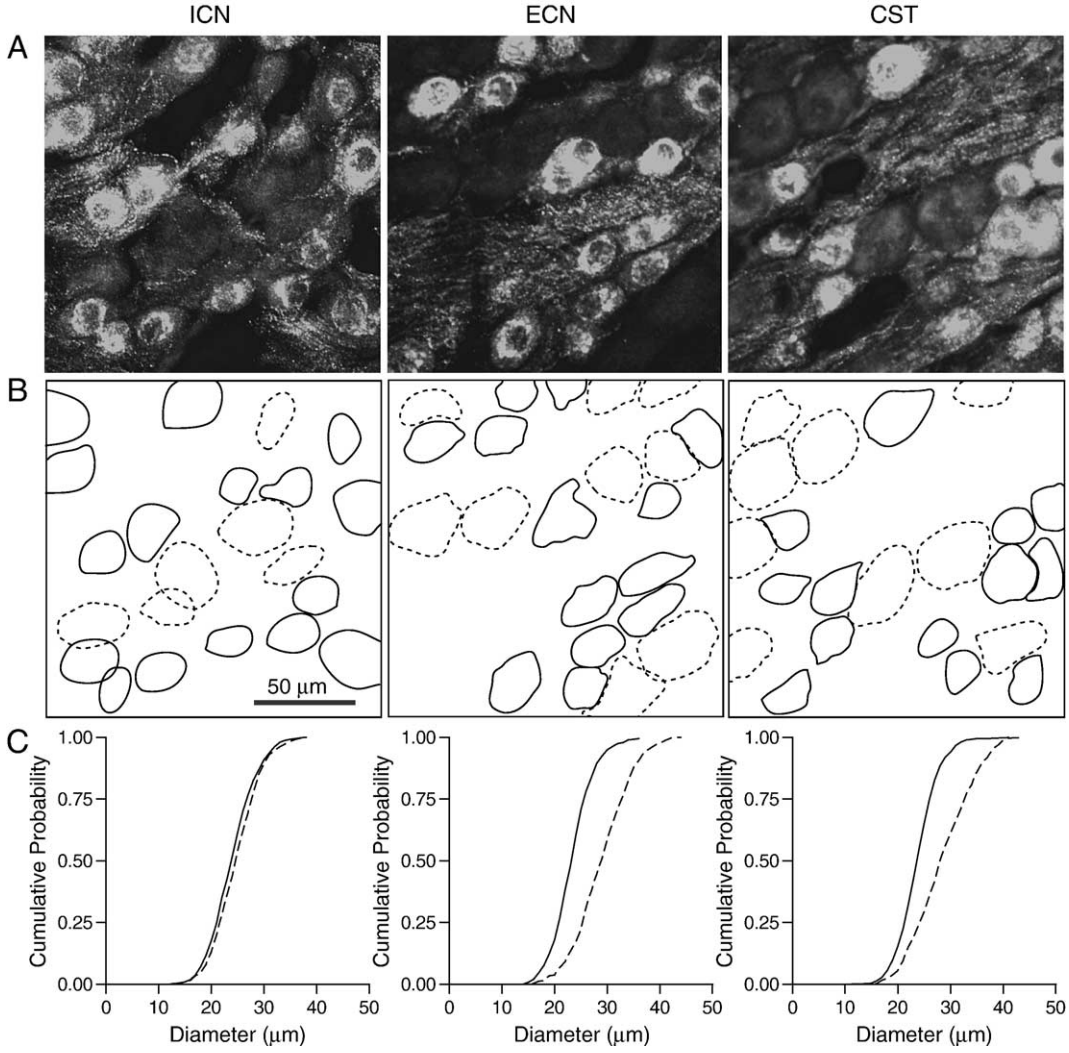

Fig. 2. Positional analysis of neuronal size and NPY-IR. (A) Photographs of NPY immunofluorescence near the ICN, ECN, and CST. (B) Drawings of cell perimeters for NPY-positive cells (solid lines) and NPY-negative cells (dashed lines). Perimeters were used to measure cell body areas and then calculate the diameters of equivalent circles. (C) Cumulative probability histograms to compare neuronal diameters of NPY-positive neurons (solid lines) and NPY-negative neurons (dashed lines). The two groups of cells are nearly identical in size near the ICN, but are quite different near the ECN and CST, where the NPY-positive cells are smaller as a group than the NPY-negative cells. The histograms were generated with pooled data from 7 SCGs in 7 animals. See Table 1 for descriptive statistics and comparisons.

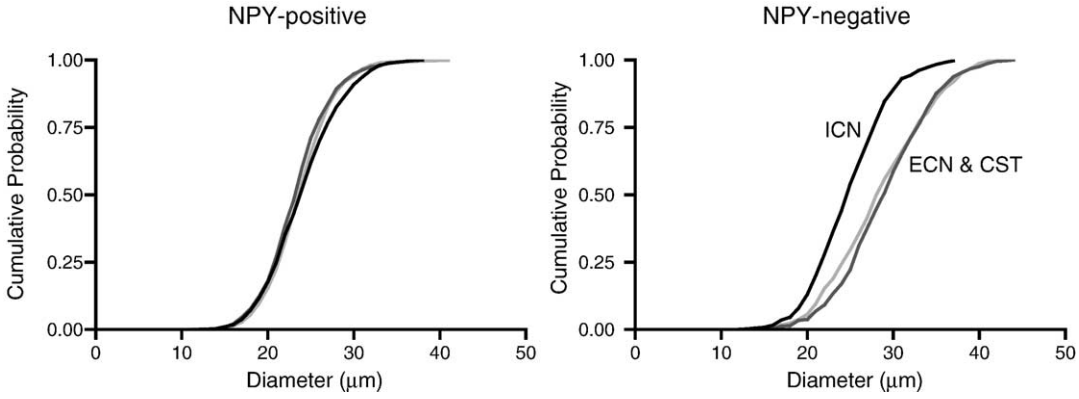

Fig. 3. NPY-negative neurons account for positional differences in neuronal size. Replotting the cumulative histograms of cell diameter from Fig. 2 to compare NPY-positive neurons at three positions (left) shows little difference between the ICN, ECN, and CST. However, comparing the histograms for NPY-negative neurons reveals the presence of larger cells in the caudal ganglion near the ECN and CST.

are virtually superimposable (Fig. 3, left). In contrast, NPY-negative neurons are clearly larger at the CST and ECN than at the ICN (Fig. 3, right). Thus, the position-dependence of size differences between NPY-positive and NPY-negative neurons is due to large NPY-negative neurons that are present in the caudal, but not the rostral, ganglion.

From previous retrograde tracing studies, it seemed likely that the large NPY-negative neurons in the caudal ganglion are secretomotor neurons projecting to the submandibular salivary glands [8,10,31]. Grkovic and Anderson (1995) have reported that these neurons are surrounded by dense baskets of calretinin-positive preganglionic fibers. When SCG sections were double-labeled for NPY (Fig. 4A) and calretinin (Fig. 4B), we found brightly stained calretinin-positive nerve fibers throughout the entire rostro-caudal extent of the SCG including the cervical sympathetic trunk, but not in the internal and external carotid nerves. As expected, there were many dense calretinin-positive baskets surrounding large NPY-negative neurons in the caudal ganglion (Figs. 4A, B), between the CST and ECN. However, we also observed numerous less elaborate contacts between calretinin-positive fibers and ganglionic neurons, some of which were NPY-positive (Figs. 4A, B). On balance, the intense level of overall fiber staining in our material made it difficult to identify unambiguously calretinin-positive baskets of nerve fibers, as opposed to more simple contacts, and use this feature as an independent criterion for classification of secretomotor neurons.

To identify another neuronal phenotype in the SCG, additional sections were stained for NPY (Fig. 4C) and calcitonin gene-related peptide (CGRP) (Fig. 4D). A relatively small population of pupillomotor sympathetic neurons that project to the iris are located in the rostral SCG, express NPY, and receive somatic contacts from

Table 1
Topographic distribution of NPY-positive and NPY-negative neurons in the SCG

Landmark	Internal carotid nerve		External carotid nerve		Cervical sympathetic trunk	
Animal #	NPY+	NPY−	NPY+	NPY−	NPY+	NPY−
Males						
1	24.7 ± 4.9 (79)	24.3 ± 4.1 (15)	22.4 ± 3.3 (73)	28.7 ± 4.8 (31)	24.7 ± 3.6 (76)	33.6 ± 4.2 (38)
2	22.5 ± 3.3 (63)	23.6 ± 3.0 (21)	23.3 ± 3.4 (77)	28.3 ± 3.7 (56)	24.6 ± 3.7 (70)	28.0 ± 5.8 (47)
3	24.8 ± 4.0 (207)	27.7 ± 4.1 (63)	25.3 ± 4.3 (146)	30.7 ± 4.6 (58)	25.1 ± 3.5 (152)	29.3 ± 5.0 (86)
4	26.0 ± 4.3 (156)	26.3 ± 4.4 (73)	25.0 ± 3.4 (140)	29.8 ± 4.7 (92)	25.2 ± 3.5 (126)	30.3 ± 5.1 (73)
5	24.7 ± 3.7 (106)	24.2 ± 4.2 (57)	24.1 ± 4.1 (84)	32.2 ± 5.8 (76)	24.2 ± 3.4 (102)	30.2 ± 5.9 (74)
Subtotals	24.9 ± 4.2 (611)	25.8 ± 4.4 (229)	24.3 ± 3.9 (520)[a]	30.2 ± 5.0 (313)	24.8 ± 3.5 (526)[a]	30.1 ± 5.4 (318)
Females						
1	22.2 ± 3.7 (122)	23.6 ± 3.9 (86)	21.2 ± 3.1 (120)	25.6 ± 5.0 (105)	21.7 ± 4.0 (148)	23.8 ± 4.5 (78)
2	24.9 ± 4.4 (139)	25.6 ± 4.3 (61)	24.4 ± 3.3 (127)	31.5 ± 4.4 (83)	24.6 ± 3.2 (118)	29.3 ± 5.0 (85)
Subtotals	23.6 ± 4.3 (261)	24.4 ± 4.1 (147)	22.8 ± 3.6 (247)	28.2 ± 5.6 (188)	23.0 ± 3.9 (266)	26.7 ± 5.5 (163)
Grand totals	24.5 ± 4.3 (872)[b]	25.2 ± 4.3 (376)	23.8 ± 3.9 (767)[a]	29.4 ± 5.3 (501)	24.2 ± 3.8 (792)[a]	28.9 ± 5.7 (481)

Cell diameters are expressed as the mean ± SD (number of profiles).
NPY+ group different from NPY− group at same location.
[a] $P < 0.001$ (ANOVA with Tukey's post test).
[b] $P < 0.01$ (ANOVA with Tukey's post test).

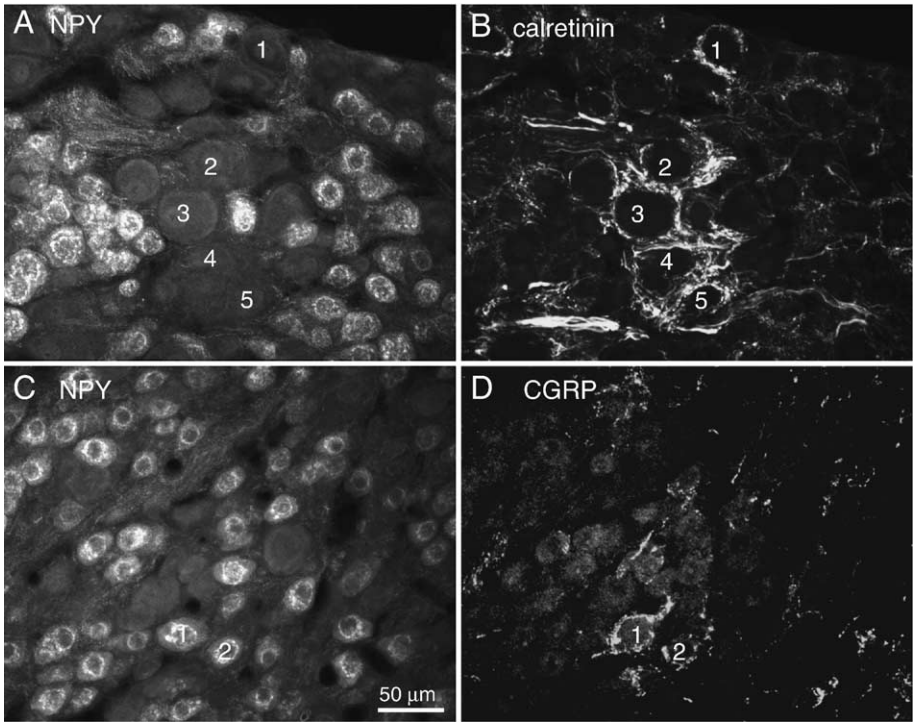

Fig. 4. Double labeling for NPY (A) and calretinin (B) and for NPY (C) and CGRP (D). Panels A and B contain examples of 5 numbered neurons that were near the CST, large, NPY-negative and surrounded by dense baskets of calretinin-positive nerve fibers. These cells are most likely secretomotor neurons projecting to salivary glands. In addition, the photographs contain more lightly labeled axons in apposition to other NPY-negative neurons and NPY-positive neurons and some neurons that are not contacted by calretinin-positive fibers. Panels C and D contain examples of 2 numbered neurons that were near the ICN, NPY-positive and contacted by CGRP-positive axonal processes, thereby identifying them as pupillomotor neurons.

CGRP-positive preganglionic fibers [8,15,32]. Consistent with these earlier observations, CGRP-positive axons in the SCG were very sparse, but could be found making contacts preferentially with occasional NPY-positive neurons (Figs. 4C, D).

4. Discussion

The results from this study indicate that almost 2/3 of the sympathetic neurons in the rat SCG express NPY, that these cells are smaller on average than NPY-negative neurons, and that the size differential between NPY-positive and NPY-negative neurons varies along the rostro-caudal axis of the ganglion. The first finding agrees with previous estimates of the size of the NPY-positive population in the rat SCG and other sympathetic ganglia [11,21]. The second finding, concerning the relatively small size of NPY-positive neurons, demonstrates a parallel with amphibian paravertebral sympathetic ganglia nine and ten and with the mouse SCG [10,17]. To our knowledge, the finding of positional variations is new, yet consistent with previous information about the unique cellular topography of the mammalian SCG. Although our experiments only included two females, there were no strong signs of sexual dimorphism, with only a weak suggestion that all sympathetic neurons may be slightly smaller in females than in males.

Our results indicate that size may serve as a practical criterion for preliminary identification of SCG cells lying caudal to the ECN, where NPY-positive neurons are 20% smaller than NPY-negative neurons. By analogy with previous studies of amphibian ganglia, it seems quite likely that under a compound microscope, one should be able to discriminate between neurons that differ by 6 or more micrometers in diameter and use this as a guide for preferential impalement of putative vasoconstrictor and pilomotor cells as opposed to secretomotor cells. For example, if one focuses upon a cell in the caudal SCG with a diameter >30 µm, then our data show the chances are 80% that it will be an NPY-negative neuron and it is also quite likely to be a secretomotor in function. If, on the other hand, one examines a neuron in the caudal SCG with a diameter <24 µm, then the chances of it being NPY-positive are 72% and such neurons are generally vasoconstrictors. Definitive identification of sympathetic phenotypes will require analysis of additional markers, such as calretinin and CGRP. In future studies, it will also be interesting to see how cell size, position, and expression of chemical markers correlate with the physiological properties of sympathetic neurons. In the longer term, a spectacular solution to the problem of neuronal identification would be the development of rodent strains with genetically coded fluorescent markers of different phenotypes.

Acknowledgment

This work was supported by NIH grant RO1 NS21065.

References

[1] D. Adams, A. Harper, Electrophysiological properties of autonomic ganglion neurons, in: E. McLachlan (Ed.), Autonomic Ganglia, Harwood Academic Publishers, Luxembourg, 1995, pp. 153–212.
[2] A.G. Blomqvist, C. Soderberg, I. Lundell, R.J. Milner, D. Larhammar, Strong evolutionary conservation of neuropeptide Y: sequences of chicken, goldfish, and *Torpedo marmorata* DNA clones, Proc. Natl. Acad. Sci. U. S. A. 89 (1992) 2350–2354.
[3] C.W. Bowers, R.E. Zigmond, Localization of neurons in the rat superior cervical ganglion that project into different postganglionic trunks, J. Comp. Neurol. 185 (1979) 381–391.
[4] C.W. Bowers, L.M. Dahm, R.E. Zigmond, The number and distribution of sympathetic neurons that innervate the rat pineal gland, Neuroscience 13 (1984) 87–96.
[5] J.M. Cerda-Reverter, D. Larhammar, Neuropeptide Y family of peptides: structure, anatomical expression, function, and molecular evolution, Biochem. Cell Biol. 78 (2000) 371–392.
[6] R.S. Chanthaphavong, S.M. Murphy, C.R. Anderson, Chemical coding of sympathetic neurons controlling the tarsal muscle of the rat, Auton. Neurosci. 105 (2003) 77–89.
[7] J. Dodd, J.P. Horn, A reclassification of B and C neurones in the ninth and tenth paravertebral sympathetic ganglia of the bullfrog, J. Physiol. 334 (1983) 255–269.
[8] D.L. Flett, C. Bell, Topography of functional subpopulations of neurons in the superior cervical ganglion of the rat, J. Anat. 177 (1991) 55–66.
[9] J.B. Furness, J.L. Morris, I.L. Gibbins, M. Costa, Chemical coding of neurons and plurichemical transmission, Annu. Rev. Pharmacol. Toxicol. 29 (1989) 289–306.
[10] I.L. Gibbins, Vasomotor, pilomotor and secretomotor neurons distinguished by size and neuropeptide content in superior cervical ganglia of mice, J. Auton. Nerv. Syst. 34 (1991) 171–183.
[11] I.L. Gibbins, Chemical neuroanatomy of sympathetic ganglia, in: E. McLachlan (Ed.), Autonomic Ganglia, Harwood Academic Publishers, Luxembourg, 1995, pp. 73–122.
[12] I.L. Gibbins, P. Jobling, J.L. Morris, Functional organization of peripheral vasomotor pathways, Acta Physiol. Scand. 177 (2003) 237–245.
[13] I.L. Gibbins, P. Jobling, E.H. Teo, S.E. Matthew, J.L. Morris, Heterogeneous expression of SNAP-25 and synaptic vesicle proteins by central and peripheral inputs to sympathetic neurons, J. Comp. Neurol. 459 (2003) 25–43.
[14] I. Grkovic, C.R. Anderson, Calretinin-containing preganglionic nerve terminals in the rat superior cervical ganglion surround neurons projecting to the submandibular salivary gland, Brain Res. 684 (1995) 127–135.
[15] I. Grkovic, S.L. Edwards, S.M. Murphy, C.R. Anderson, Chemically distinct preganglionic inputs to iris-projecting postganglionic neurons in the rat: a light and electron microscopic study, J. Comp. Neurol. 412 (1999) 606–616.
[16] J.P. Horn, W.D. Stofer, Preganglionic and sensory origins of calcitonin gene-related peptide-like and substance P-like immunoreactivities in bullfrog sympathetic ganglia, J. Neurosci. 9 (1989) 2543–2561.
[17] J.P. Horn, W.D. Stofer, S. Fatherazi, Neuropeptide Y-like immunoreactivity in bullfrog sympathetic ganglia is restricted to C cells, J. Neurosci. 7 (1987) 1717–1727.
[18] L.Y. Jan, Y.N. Jan, Peptidergic transmission in sympathetic ganglia of the frog, J. Physiol. 327 (1982) 219–246.
[19] Y.N. Jan, L.Y. Jan, S.W. Kuffler, A peptide as a possible transmitter in sympathetic ganglia of the frog, Proc. Natl. Acad. Sci. U. S. A. 76 (1979) 1501–1505.
[20] W. Janig, E.M. McLachlan, Specialized functional pathways are the building blocks of the autonomic nervous system, J. Auton. Nerv. Syst. 41 (1992) 3–13.
[21] R. Jarvi, P. Helen, M. Pelto-Huikko, A. Hervonen, Neuropeptide Y (NPY)-like immunoreactivity in rat sympathetic neurons and small granule-containing cells, Neurosci. Lett. 67 (1986) 223–227.
[22] P. Jobling, I.L. Gibbins, Electrophysiological and morphological diversity of mouse sympathetic neurons, J. Neurophysiol. 82 (1999) 2747–2764.
[23] P. Jobling, J.P. Horn, In vitro relation between preganglionic sympathetic stimulation and activity of cutaneous glands in the bullfrog, J. Physiol. 494 (Pt. 1) (1996) 287–296.
[24] J.L. Morris, S. Nilsson, The circulatory system, in: S. Holmgren (Ed.), Comparative Physiology and Evolution of the Autonomic Nervous System, Harwood Academic Publishers, Chur, Switzerland, 1994, pp. 193–246.
[25] J.L. Morris, I.L. Gibbins, G. Campbell, R. Murphy, J.B. Furness, M. Costa, Innervation of the large arteries and heart of the toad (*Bufo marinus*) by adrenergic and peptide-containing neurons, Cell Tissue Res. 243 (1986) 171–184.
[26] S. Nishi, H. Soeda, K. Koketsu, Studies on sympathetic B and C neurons and patterns of pregnaglionic innervation, J. Cell. Physiol. 66 (1965) 19–32.
[27] S. Reuss, R.Y. Moore, Neuropeptide Y-containing neurons in the rat superior cervical ganglion: projections to the pineal gland, J. Pineal Res. 6 (1989) 307–316.
[28] W.X. Shen, J.P. Horn, Presynaptic muscarinic inhibition in bullfrog sympathetic ganglia, J. Physiol. 491 (Pt. 2) (1996) 413–421.
[29] P.A. Smith, Amphibian sympathetic ganglia: an owner's and operator's manual, Prog. Neurobiol. 43 (1994) 439–510.
[30] R. Thorne, J.P. Horn, Role of ganglionic cotransmission in sympathetic control of the isolated bullfrog aorta, J. Physiol. 498 (Pt. 1) (1997) 201–214.
[31] J.T. Voyvodic, Peripheral target regulation of dendritic geometry in the rat superior cervical ganglion, J. Neurosci.0 9 (1989) 1997–2010.
[32] K. Yamamoto, E. Senba, T. Matsunaga, M. Tohyama, Calcitonin gene-related peptide containing sympathetic preganglionic and sensory neurons projecting to the superior cervical ganglion of the rat, Brain Res. 487 (1989) 158–164.